Quaternary Research 84 (2015) 223–231

Contents lists available at ScienceDirect

Quaternary Research

journal homepage: www.elsevier.com/locate/yqres

Vegetation responses to the last glacial and early Holocene environmental changes in the northern Leizhou Peninsula, south China

Jibin Xue [a,*], Wei Zhong [a], Lichun Xie [b], Ingmar Unkel [c]

[a] School of Geographical Sciences, South China Normal University, Guangzhou 510631, China
[b] School of Geography and Tourism, Guangdong University of Finance & Economics, Guangzhou 510320,China
[c] Institute for Ecosystem Research, Kiel University, Olshausenstr. 75, Kiel D-24118 Germany

ARTICLE INFO

Article history:
Received 20 September 2014

Keywords:
Pollen analysis
Vegetation change
Peat
Last glacial period
Leizhou Peninsula

ABSTRACT

A well-dated palynological record spanning the interval ~40,500–7060 cal yr BP, retrieved from a peatland on the Leizhou Peninsula in south China, clearly shows regional vegetation and climate changes during the last glacial period. Pollen data showed that the study region was mainly covered by subtropical evergreen trees during Marine Isotope Stage 3 (MIS 3), indicating a subtropical climate with relatively high temperature and precipitation. During MIS 2, subtropical evergreen-deciduous forest with large areas of grassland occurred, implying cooler and drier conditions. Some tropical forest elements increased during the early Holocene, indicating a warm and wet trend. Several millennial-scale oscillations of the pollen records appeared to correlate with the cold anomalies in the North Atlantic region. Our records agree well with many records from other regions, but they are a bit different than that inferred from the neighboring Huguang Maar Lake. Furthermore, our results suggest that the vegetation surrounding Xialu peatland was strongly influenced by the migration of the intertropical convergence zone (ITCZ) and variability in the East Asian summer monsoon (EASM). Changes of atmospheric CO_2 concentration (pCO_2) levels may have also affected the long-term vegetation changes in the study region.

© 2015 University of Washington. Published by Elsevier Inc. All rights reserved.

Introduction

Ecosystems are dynamic, responding to changes in climate and other environmental factors. Simulations with dynamic global vegetation models have shown changes in vegetation distribution in response to transient changes in climate and atmospheric CO_2 during the 21st century (Harrison and Sanchez-Goñi, 2010). Hence, understanding past long-term vegetation responses to regional or even global environmental changes in terms of time scales and forcing mechanisms is quite essential to future climate change projections, because the response of vegetation to climate changes appears to vary among regions and times. However, in tropical low-latitude south China, high-resolution records of terrestrial vegetation changes and their possible responses to environmental changes since the last glacial period are still lacking, and the evolution of vegetation and climate changes during this time still remains controversial (Liu and Wang, 2004; Sun and Luo, 2004; Liu, 2007; Xue et al., 2014).

The northern Leizhou Peninsula is located in the transitional zone between the tropical and south subtropical subzones in south China (Fig. 1). Numerous field investigations during the last several years indicate that there are many peatlands preserved on the Leizhou Peninsula, with some containing records that extend back 41,000 yr (Xue et al., 2014). These sites are well suited to investigate long-term vegetation and environmental history, because multiple proxy data from peat records (e.g., palynological data, degree of peat decomposition) can potentially be used to reconstruct regional vegetation and climate patterns (Blackford, 2000; Kamenik et al., 2009; Zhao et al., 2011). In recent years, many palynological investigations from lake sediments in Leizhou Peninsula have provided valuable information on paleovegetation, paleoclimate, and monsoonal evolution in south China (e.g., Zheng and Lei, 1999; Fuhrmann et al., 2003; Mingram et al., 2004; Wang et al., 2012), and a 4–6°C decrease of mean annual temperature (MAT) during the last glacial period in this region has been estimated (Zheng and Lei, 1999; Wang et al., 2012). However, few studies have used peat sediments to infer paleovegetation and paleoclimate changes in this area (but see Xue et al., 2014). In particular, a previous study has suggested that there were differences in the regional patterns of C_3 and C_4 vegetation changes at different sites in the Leizhou Peninsula since the last glacial period (Xue et al., 2014). Therefore, more detailed studies from different sites are needed to better address the paleovegetation changes in this region, and develop a more spatially resolved perspective on past changes.

In this study, we present a detailed pollen record from the 210-cm sediment core XL02 recovered from the Xialu peatland at the northern Leizhou Peninsula. Results of the pollen-based vegetation reconstruction are then used to discuss late Quaternary vegetation changes and

* Corresponding author.
E-mail address: jbxue@scnu.edu.cn (J. Xue).

http://dx.doi.org/10.1016/j.yqres.2015.08.001
0033-5894/© 2015 University of Washington. Published by Elsevier Inc. All rights reserved.

https://doi.org/10.1016/j.yqres.2015.08.001 Published online by Cambridge University Press

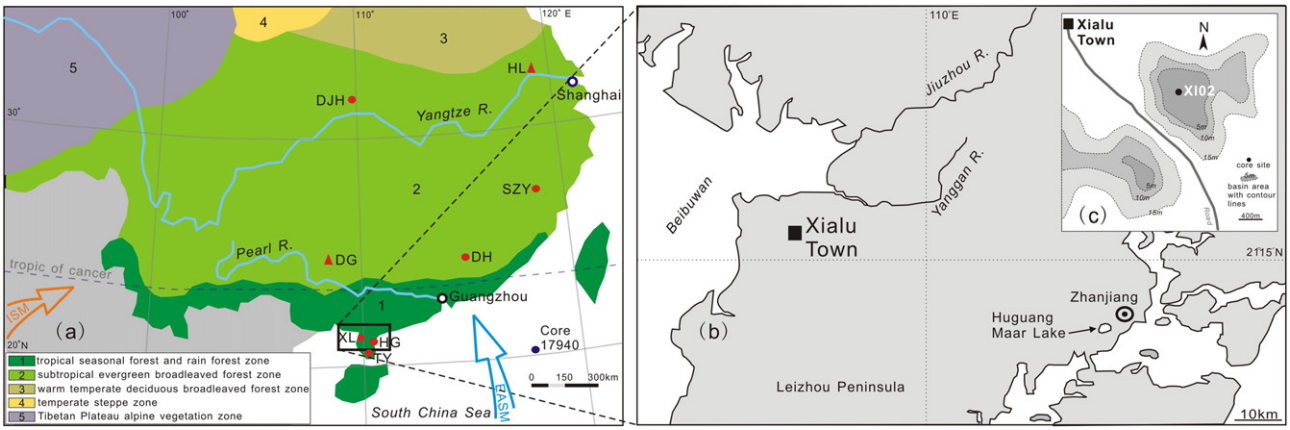

Figure 1. Map of the modern vegetation zones in southern China and the location of core XL02. Some key sites mentioned in the text are also shown. HL: Hulu Cave (Wang et al., 2001); DG: Dongge Cave (Dykoski et al., 2005); HG: Huguang Maar Lake (Fuhrmann et al., 2003; Mingram et al., 2004); TY: Tiangyang volcanic basin (Zheng and Lei, 1999); DH: Dahu swamp (Zhong et al., 2010); SZY: SZY peat bog, Pingnan county (Yue et al., 2012); DJH: Dajiuhu peat bog (Li et al., 2013); Core 17940: deep-core from the South China Sea (Sun and Li, 1999).

assess the implications of these records for regional climate change and ecosystem response since the last glacial period.

Study area and regional setting

The Xialu peatland is situated on the coastal area of northern Leizhou Peninsula (Fig. 1), with an elevation of approximately 5–8 m above sea level. To date no evidence has indicated a higher sea level since the last glacial period that could affect the sampling site. Sea level is generally considered to have fallen by tens of meters during the last glacial period (Siddall et al., 2008), and the sea level in South China Sea was about 100–120 m below present at the last glacial maximum (LGM) (Lambeck and Chappell, 2001). Even in the mid-Holocene, when the sea level reached its highest after the last glacial, the sea level on the southwestern Leizhou Peninsula stood only about 2–3 m higher than at present (Yu et al., 2002). Thus, we deduce that the sampling site has not been influenced by sea-level fluctuations since the last glacial period.

The climate in this region is controlled by the warm/humid EASM and to a lesser extent by the Indian summer monsoon (ISM) in the summer season, as well as the cold/dry north winds from the Siberian–Mongolian High in the winter season (i.e., the winter monsoon) (Fuhrmann et al., 2003; Herzschuh, 2006). The studied area has a mean annual precipitation (MAP) of about 1600 mm, most of which occurs in the summer season (mainly from April to October) in association with the EASM, and a MAT of about 23°C (Fig. 2). Modern natural vegetation mainly belongs to the tropical semi-evergreen seasonal rain forest (Zheng and Lei, 1999). On the dry land and hill slopes, open forests and tropical grassland are widespread, and dominated by Poaceae species and heliophytic ferns such as *Dicranopteris*. A few semi-natural forests occupy the hills and are composed mainly of *Ficus*, *Syzygium*, *Elaeocarpus*, *Antidesma*, *Artocarpus* and *Antiaris*. Due to strong human disturbances, there are only small relicts of the original flora left in this region today.

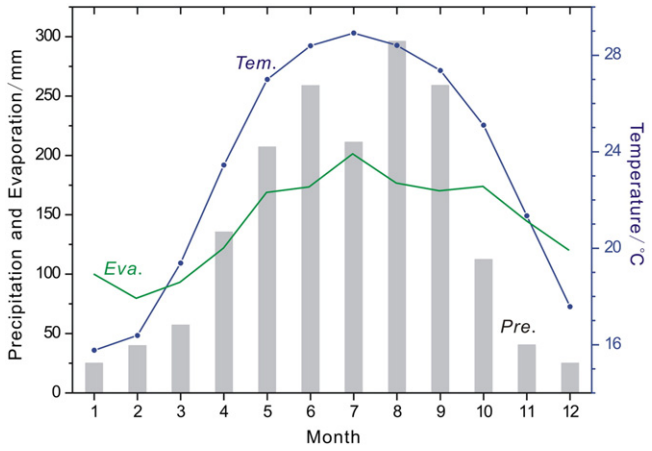

Figure 2. Mean monthly temperature, precipitation and evaporation from Zhanjiang climate station during AD 1960–2008 AD (data from Guangdong Meteorological Bureau).

Materials and methods

In May 2006, several cores were recovered from the Xialu peatland (21°18′N, 109°49′E; Fig. 1), using a Russian peat corer (chamber 500 mm long, 75 mm diameter). Twin boreholes were drilled at the same sampling site and the cores overlapped at least by 30 cm. The stratigraphy was recorded initially in the field and was described in further detail when they were opened for sampling in the lab.

In this study, 58 pollen samples of ~1 cm^3 were analyzed at 3-cm intervals from the 30- to 200-cm section of the XL02 core. Samples for pollen analysis were processed using heavy liquid separation (Nakagawa et al., 1998). In brief, the preparation procedures involve treatments with 10% HCl to remove carbonates, 10% KOH to remove humic substances, heavy liquid floatation (a $ZnCl_2$ solution was used heaving a specific gravity of between 2.0 and 2.2), acetolysis to remove cellulose, followed by mounting the sample in a glycerin jelly. One tablet of *Lycopodium* marker spores was added to each sample for calculating total pollen and spore concentrations. Pollen identification was aided with references (Institute of Botany and South China Institute of Botany, Academic Sinica, 1982; Wang et al., 1995). At least 300 pollen and spores were counted for each sample. All samples were identified at the Key Laboratory of Marginal Sea Geology, Chinese Academy of Sciences (CAS). Pollen percentages were calculated based on the total terrestrial pollen sum, and stratigraphic zones were assigned by a stratigraphically constrained cluster analysis using CONISS (Grimm, 1987). To summarize patterns of palynological change, eleven pollen taxa with average percentages >1.5% were used for principal component analysis (PCA) using the software DPS v7.05 (Tang and Zhang, 2013). Other proxies from the same core, including loss on ignition (LOI), organic matter content (OM), humification degree of peat (HD), and organic carbon stable isotope ($\delta^{13}C_{org}$), have also been measured and presented in an earlier study (Xue et al., 2014).

Eight samples were ^{14}C dated using both conventional and AMS techniques at the radiocarbon dating laboratory of Lanzhou University and Peking University, respectively (Table 1). An age–depth model was developed after calibration of these radiocarbon dates with the

https://doi.org/10.1016/j.yqres.2015.08.001 Published online by Cambridge University Press

Table 1
List of radiocarbon dates for core XL02.

Laboratory no.	Sample depth (cm)	^{14}C age (yr BP)	Calibrated age (cal yr BP)	Materials	Dating method
LUG12-111	30–35	7232 ± 99	8168–7981	Peat	Conv.
LUG06-20	50–60	10789 ± 106	12814–12635	Peat	Conv.
LAMS0728	65–66	14000 ± 55	17122–16895	Plant remains	AMS
LUG06-21	70–80	17822 ± 151	21550–21096	Peat	Conv.
LAMS0741	120–121	25585 ± 135	30001–29523	Plant remains	AMS
LUG06-23	130–140	29930 ± 351	33445–32729	Peat	Conv.
LUG12-106	180–185	33636 ± 224	38528–38095	Peat	Conv.
LUG06-24	200–210	35942 ± 398	41471–40832	Peat	Conv.

IntCal13 calibration curve (Reimer et al., 2013) using OxCal 4.2 (Bronk, 2008, 2009; Table 1, Fig. 3). An age–depth curve was directly extracted from the OxCal model, returning maximal and minimal ages for every 1 cm interval. A curve based on the mean age values [(age_{max} + age_{min}) / 2] was then used to plot the proxy data of the core. All ages are reported with the 1-sigma (68.2%) probability range, and are denoted as calibrated years BP (before AD 1950).

Results

Sediment lithology and chronology

The XL02 peat core is mainly composed of two sedimentary units (Fig. 3): Unit 2 (210–105 cm) consists of 105 cm of fairly highly humified dark-brown-colored peat, with relatively higher values of LOI, HD and OM; Unit 1 (105–27 cm) consists of 78 cm of fairly weakly humified yellowish and light-brown-colored peat, with relatively lower values of LOI, HD and OM (data missing from 40–30 cm). The two sedimentary units show obviously different accumulation rates, with ~64 mm/ka from 210 to 105 cm in depth in Unit 2, followed by significantly decreased accumulation rate from 105 to 27 cm in Unit 1 of ~37 mm/ka. It should be noted that many tree remains occur from 105 to 90 cm and from 180 to 165 cm. The chronology indicates that the peat core covers the interval ~40,500–7060 cal yr BP. The mean sediment accumulation rate was ~5.4 cm/ka, and the temporal sampling resolution is thus currently ~180 yr per sample for the fossil pollen record.

Pollen assemblages

A total of 78 pollen and spore types were identified from the 58 pollen samples, including 52 arboreal taxa, 17 herbaceous taxa, 6 fern taxa, and 3 types of moss and algal palynomorphs; only the most abundant taxa are shown in Fig. 4. To make the pollen diagram easier to interpret, several groups of taxa are shown in Table 2 according to their ecology and modern distribution (Wang et al., 2012; Yue et al., 2012). The identified taxa mainly derived from tropical, subtropical and temperate vegetation types, and the samples were especially rich in pollen from subtropical species (Fig. 5). The tropical and subtropical broad-leaved taxa included *Altingia*, *Ilex*, evergreen *Quercus* (*Quercus* (E.)), *Castanopsis*/*Lithocarpus* (*Cast./Lith.*), Moreaceae, and *Mallotus*. The temperate broad-leaved taxa included *Fagus*, *Corylus*, deciduous *Quercus* (*Quercus* (D.)), Ericaceae, and *Alnus*. The montane conifer taxa included *Pinus*, *Tsuga* and *Abies*. The main components of herb pollen were Poaceae, *Artemisia*, Cyperaceae and Liliaceae. The ferns were mainly represented by Monolete-spores and *Lycopodium*. Arboreal pollen (AP) percentages were commonly greater than the non-arboreal ones (NAP) in MIS 3 and the early Holocene, while the AP percentages were less than the NAP ones in MIS 2 (Fig. 5). Based on the results of CONISS, the pollen record was divided into 3 pollen assemblage zones, with subzones when necessary (Fig. 4).

Zone 1 (200–123 cm, ~40,500–30,400 cal yr BP): Pollen assemblages of Zone 1 were dominated by *Altingia* (averaging 35%), *Quercus* (E.) (12%), *Sapindaceae* (7%) and Poaceae (33%). *Altingia* had the highest abundance within this zone (up to 51%) of the entire core. Pollen percentages of subtropical arboreal taxa and herbaceous taxa were 60% and 35%, respectively. The ratio of AP percentages to NAP ones (AP/NAP) was relatively high (ranging from 0.4 to 5.4, mean of 2.8) and fluctuated markedly.

Zone 2 (123–69 cm, 30,400–19,100 cal yr BP): Pollen assemblages of Zone 2 were characterized by *Altingia* (17%), *Quercus* (E.) (35%), *Cast./Lith.* (10%), *Sapindaceae* (8%) and Poaceae (19%). In this zone, *Quercus* (E.) and *Cast./Lith.* increased markedly to the highest levels in the core

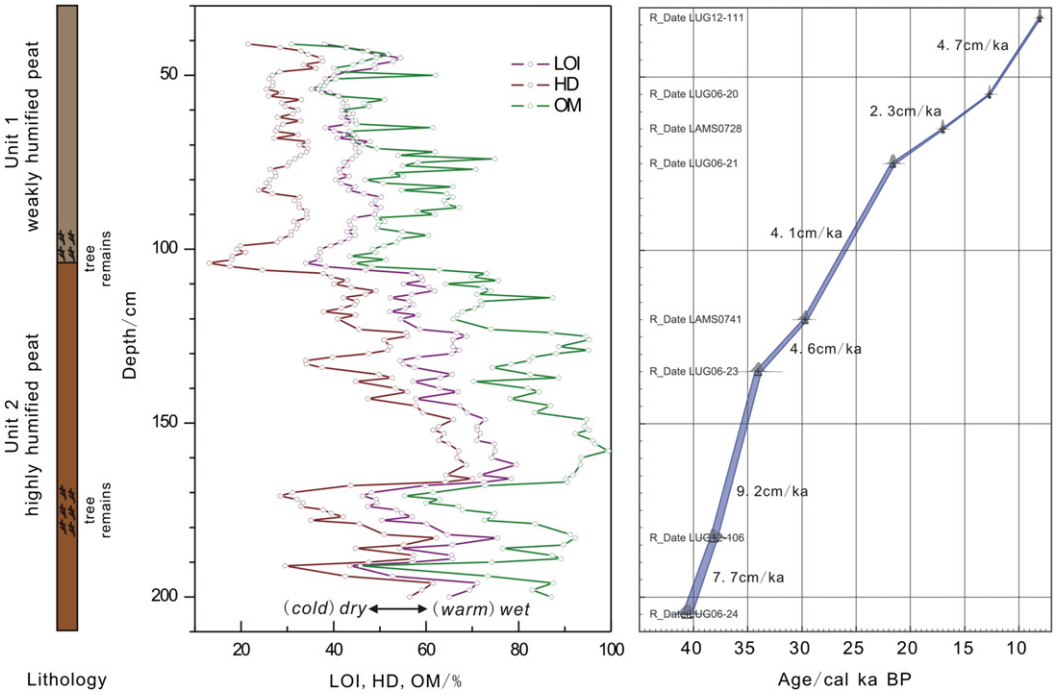

Figure 3. Age–depth model and sediment lithology.

https://doi.org/10.1016/j.yqres.2015.08.001 Published online by Cambridge University Press

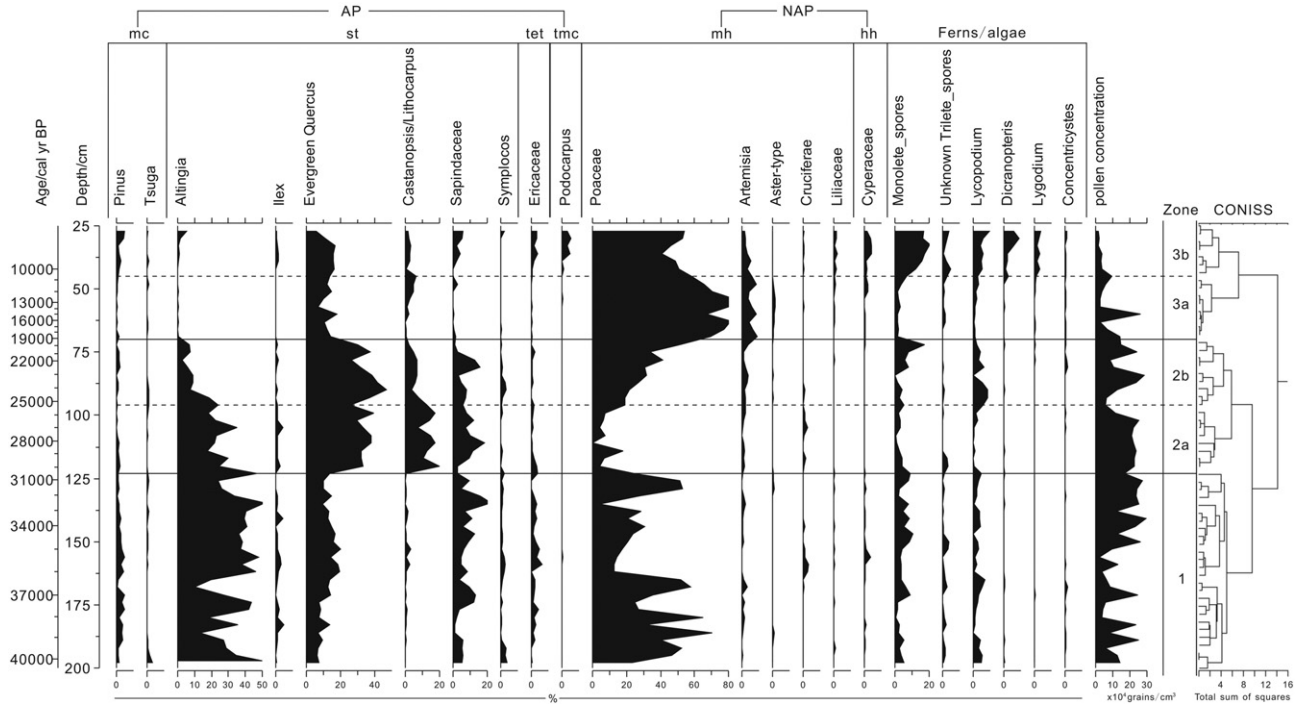

Figure 4. Pollen diagram of key pollen types from core XL02.

(up to 47% and 17%, respectively), while *Altingia* started to decline gradually. The AP percentages, AP/NAP, and pollen percentage of the subtropical arboreal taxa reached their maximums during this period, and Poaceae and the pollen percentage of herbaceous taxa reached their minimums. Two subzones were separated at about 96 cm (~25,300 cal yr BP), mostly based on the decrease in *Altingia* and increase in Poaceae.

Zone 3 (69–27 cm, 19,100–7060 cal yr BP): Pollen assemblages of Zone 3 were mainly characterized by high Poaceae (63%) and relatively high *Quercus* (E.) (13%). *Artemisia* also slightly increased compared to the former two zones. Pollen percentages of the AP and subtropical arboreal taxa reached their minimum values of 10% and 11%, respectively, while the Poaceae and herbaceous taxa maintained at highest levels in the entire core. The AP/NAP also reached its minimum values (0.11) and maintained a consistently low level in this zone. Two subzones were divided at about 45 cm (~10,600 cal yr BP) based mostly on the decrease in Poaceae and obvious increases in spores and ferns. Total pollen concentration was at its lowest value of the entire record.

Numerical analysis of pollen data

PCA results of eleven pollen types with percentages >1.5% summarize the main patterns of variability in the pollen data. The first two principal components (axes 1 and 2) capture 53.5% and 23.5% of the total variance, respectively (Fig. 6). PCA axis 1 (PCA-F1) mostly reflects the relative abundances of subtropical evergreen trees (*Altingia*, *Ericaceae*, *Sapindaceae* and *Quercus* (E.)) (on the right side with positive values) and herbs (Poaceae and *Artemisia*) (on the left side with negative values). It is likely that PCA-F1 mainly represents vegetation changes associated with precipitation, since more precipitation (corresponding to relatively humid conditions) can favor the growth of subtropical evergreen trees, while less precipitation (corresponding to relatively drier conditions) can favor the expansion of the steppe (or grassland). Thus, PCA-F1 can be mainly interpreted as precipitation changes from more (the positive side) to less (the negative side).

The interpretation of PCA-F2 seems a bit complex, as subtropical evergreen trees and herbaceous plants are found on both sides. However, Poaceae is positively correlated with PCA-F2, whereas the QCLS (the sum of *Quercus* (E.) + *Cast./Lith.* + *Sapindaceae*) is more negatively correlated with PCA-F2. Considering the relatively higher pollen percentages of Poaceae (ranging from 4% to 82%, mean of 37%) and QCLS (ranging from 8% to 74%, mean of 29%) throughout the entire core and their different ecological characteristics (e.g., photosynthetic pathways), PCA-F2 may represent a response to variability in atmospheric pCO_2. C_4 plants have a competitive advantage under low pCO_2

Table 2
Ecological groups of some pollen taxa.

Ecological groups	Selected pollen taxa
Montane conifers (mc)	*Abies*, *Pinus*, *Tsuga*
Tropical montane confiers (tmc)	*Dacrydium*, *Podocarpus*
Tropical trees (trt)	*Alchornea*, *Aporosa*, Euphorbiaceae, *Elaeocarpus*, *Ficus*, *Mallotus*, Moraceae, *Phyllanthus*, *Pterolobium*, Palmae, *Randia*
Subtropical trees (st)	*Altingia*, Anacardiaceae, *Castanopsis/Lithocarpus*, *Engelhardia*, Hamamelidaceae, *Ilex*, *Liquidambar*, *Myrica*, Oleaceae, *Quercus*(E.), Rutaceae, *Sapindaceae*, *Symplocos*
Temperate trees (tet)	*Alnus*, *Betula*, *Carpinus*, *Castanea*, *Celastraceae*, *Corylus*, Ericaceae, *Juglans*, *Quercus* (D.), *Ulmus*
Moderate herbs (mh)	*Artemisia*, Compositae, Cruciferae, Chenopodiaceae, Liliaceae, Poaceae, *Polygonum*
Hygrophyte herbs (hh)	*Acorus*, Alismataceae, Cyperaceae, Lythraceae, *Typha*
Ferns/algae	*Lycopodium*, *Lygodium*, Monolete-spores, *Polypodium*

https://doi.org/10.1016/j.yqres.2015.08.001 Published online by Cambridge University Press

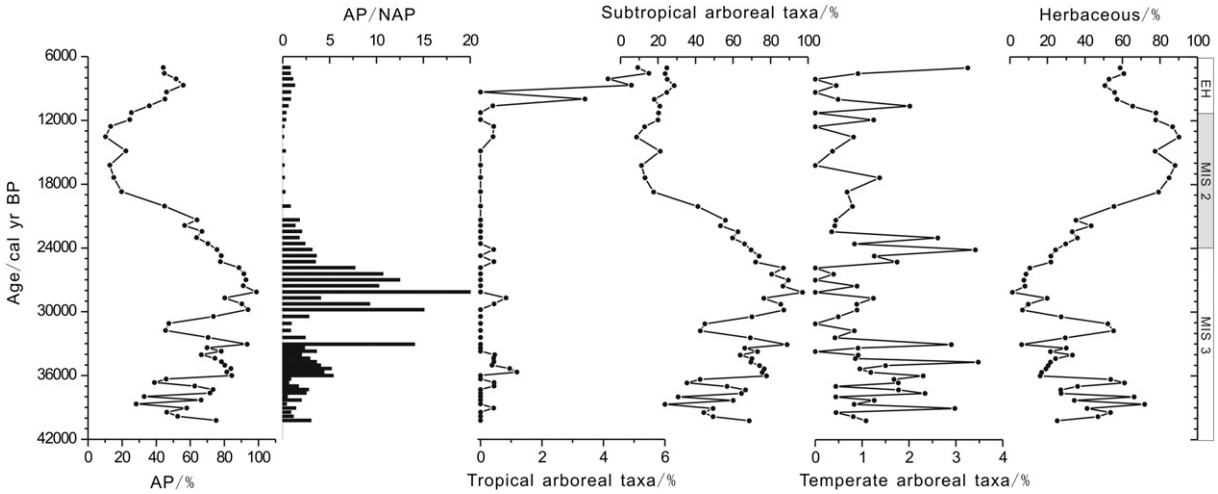

Figure 5. Key pollen groups of core XL02.

conditions due to their CO_2 concentrating mechanism, and have greater water-use efficiency than C_3 plants (e.g., *Quercus* (E.), *Cast./Lith.*, *Sapindaceae*) (Cerling et al., 1997; Huang et al., 2001). However, C_3 plants could have increased in abundance relative to C_4 plants at the low atmospheric pCO_2 levels of the last glacial period if precipitation was sufficiently high (Schefuß et al., 2003). Thus, it is possible that the PCA-F2 reflects the relative changes in pCO_2 level, to a certain extent coupled with precipitation changes during the last glacial period, although other environmental factors cannot be ruled out.

Discussion

Vegetation and climate changes during the last glacial period and early Holocene

Pollen grains deposited on the study site would have been transported chiefly by winds and rivers from the Leizhou Peninsula and its adjacent areas, including the coast areas of south China. In addition, as the sea level in South China Sea was about 100–120 m below present at the LGM (Lambeck and Chappell, 2001), the exposed South China Sea shelf may have been a minor pollen source area for the study site during the last glacial period (especially during the LGM). The pollen results from the Xialu peatland show several major changes in vegetation occurred in this region during the last glacial period and early Holocene, and were characterized by variability in the occurrence and abundance of moisture-sensitive taxa. In brief, the vegetation reconstructed from the pollen results of core XL02 is mainly characterized by obvious alternations of subtropical evergreen trees and herbs, temperate arboreal taxa never exceeded 5% in the record, and tropical arboreal taxa rose abruptly in the early Holocene (Figs. 4 and 5).

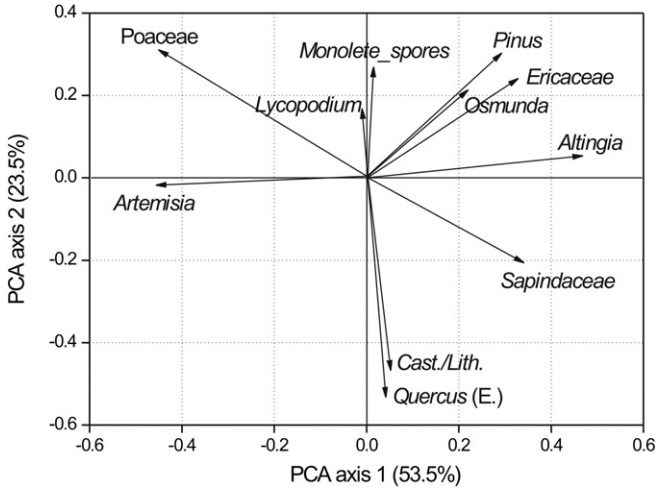

Figure 6. Biplot of PCA results from fossil pollen data from core XL02.

During MIS 3 (~40,500–24,000 cal yr BP in this study), the region was dominated by subtropical evergreen trees, mixed with a few temperate deciduous broad-leaved trees and some herbs. Tropical evergreen trees occurred only sporadically. The most abundant trees were *Altingia*, *Quercus* (E.), *Cast./Lith.* and *Sapindaceae*, with *Altingia* the most abundant (up to 51%) in the core. The modern distribution of *Altingia* in China is normally limited to the tropical and subtropical mountains (Yue et al., 2012); for instance *Altingia gracilipe* is considered a principal element in modern monsoon evergreen forest in south China located between *ca*. 500 m and 1000 m, where it is associated with *Quercus* (E.), *Cast./Lith.*, and *Schima*. Zheng and Lei (1999) reported that *Altingia* mainly occurs in modern tropical lower montane forests of Hainan Island (>800 m), where the MAP can reach about 2500 mm. For comparison, Zhanjiang, the nearest station to Xialu peatland, reports a MAP of ~1700 mm (Fig. 1b). Both *Quercus* (E.) and *Cast./Lith.* also suggest warm and wet conditions (Zhou et al., 2004). The relatively higher abundance of AP and the dominance of *Altingia*, *Quercus* (E.) and *Cast./Lith.* (Figs. 4 and 5), together with relatively higher PCA-F1 values (Fig. 7), collectively suggest that the study region was dominated by subtropical evergreen trees, indicating a subtropical climate during MIS 3.

However, the pollen record suggests that there was considerable environmental variability during MIS 3. For example, pollen assemblages indicate more subtle changes in vegetation around 40,500–36,000 cal yr BP and around 32,000–30,500 cal yr BP, when relatively higher abundances of Poaceae and herbaceous taxa, and lower values of *Altingia* and total AP occurred, implying somewhat cooler and drier conditions during these periods. A very warm and wet climate during the later period of MIS 3, from ~30,000 to ~25,300 cal yr BP (Zone 2a), also occurred and was characterized by a dramatic increases of *Quercus* (E.) and *Cast./Lith.*, and maximal values of both AP percentage and AP/NAP. At the same period, the occurrence of some drought-tolerant herbaceous taxa (e.g., Poaceae) dropped to the lowest levels in the record, perhaps due to the abundant precipitation during this interval (Fig. 7).

During the transition from MIS 3 to MIS 2 (between ~26,000 and ~21,000 cal yr BP), the AP percentage declined markedly while the NAP percentage concurrently increased (Fig. 5). This obvious transition likely reflects a response to a climatic change from relatively warmer and wetter to cooler and drier conditions, and may reflect the onset of

https://doi.org/10.1016/j.yqres.2015.08.001 Published online by Cambridge University Press

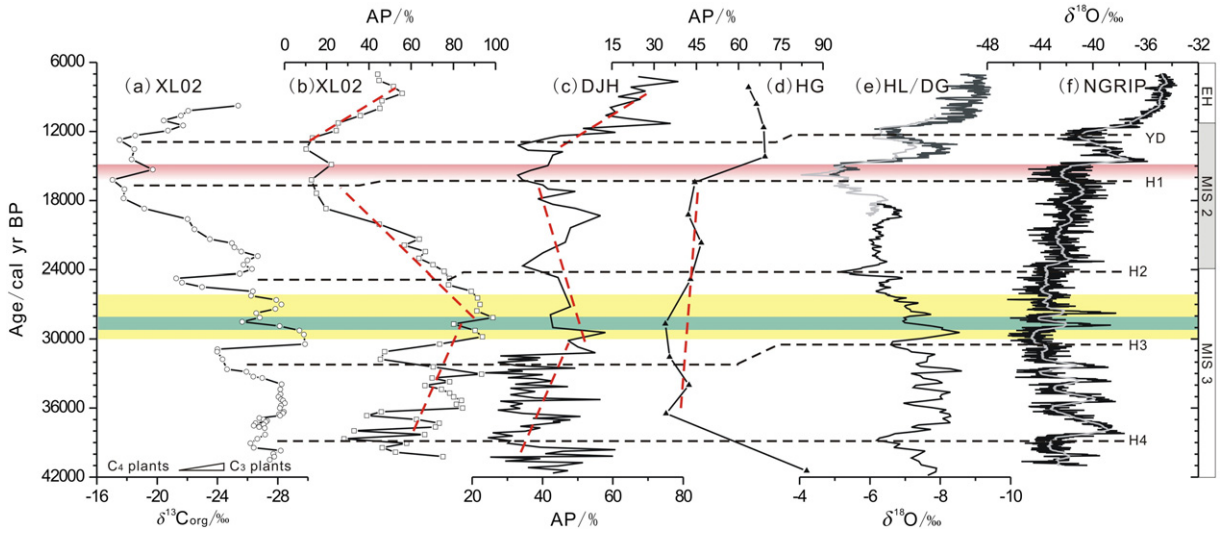

Figure 7. Regional climatic correlations. (a) $\delta^{13}C_{org}$ record from core XL02 (Xue et al., 2014); (b) AP percentage from core XL02; (c) AP percentage from Dajiuhu peatland (DJH) in central China (Li et al., 2013); (d) AP percentage from Huguang Maar lake (HG) in south China (Fuhrmann et al., 2003); (e) $\delta^{18}O$ records from Hulu and Dongge Caves (HL/DG) in China (Wang et al., 2001; Dykoski et al., 2005); (f) $\delta^{18}O$ record from NGRIP ice core (NGRIP members, 2004). The yellow-shaded band indicates a very warm and wet climate period embedded by a weaker summer monsoon event (blue-shaded band). The pink-shaded band implies a rapid warming around 16,000–15,000 cal yr BP.

the LGM (21 ± 2 ^{14}C ka BP; Peterson et al., 1979; Mix et al., 2001). Numerous geological records show that both temperature and precipitation during the LGM changed significantly, and altered vegetation composition (Wang et al., 2012). During MIS 2 (between ~24,000 and ~11,500 cal yr BP), subtropical evergreen trees, such as *Quercus* (E.) and *Cast./Lith.*, gradually decreased. Temperate trees were dominated by *Quercus* (D.) (<10%) with Ericaceae (<5%), and tropical trees almost disappeared. Poaceae and *Artemisia* reached their maximums at the same time suggesting expansion of local steppe or grassland, and likely not only a cooler, but also a much drier climate (Zheng and Lei, 1999). The rapid increase in herbs, together with relatively low PCA-F1 (Fig. 7) values, suggests a subtropical evergreen-deciduous broad-leaved forest with large areas of grassland occurred around the depositional basin during MIS 2, clearly implying cooler and drier conditions relative to MIS 3. In addition, the pollen concentration in the sediment was relatively low during MIS 2, consistent with sparse vegetation cover in the study area. The MAT for subtropical evergreen-deciduous broad-leaved forest in China today is about 18–20°C (Editorial Committee for Physical Geography of China, 1985), suggesting a 4–5°C decrease (or even more) of MAT in the northern Leizhou Peninsula during MIS 2.

A noticeable vegetation change occurred in the early Holocene (between 11,500 and 7060 cal yr BP), which was characterized by a rise of tropical forest elements and a gradual increase of subtropical forest elements (Fig. 5). At the same time, Poaceae species were still a dominant component of the vegetation. The PCA-F1 value also rose significantly (Fig. 8). Concurrently, some hygrophyte herbs and ferns began to increase, indicating the formation of local wetland. Thus, there was likely a warm and wet trend from the end of MIS 2 through the early Holocene.

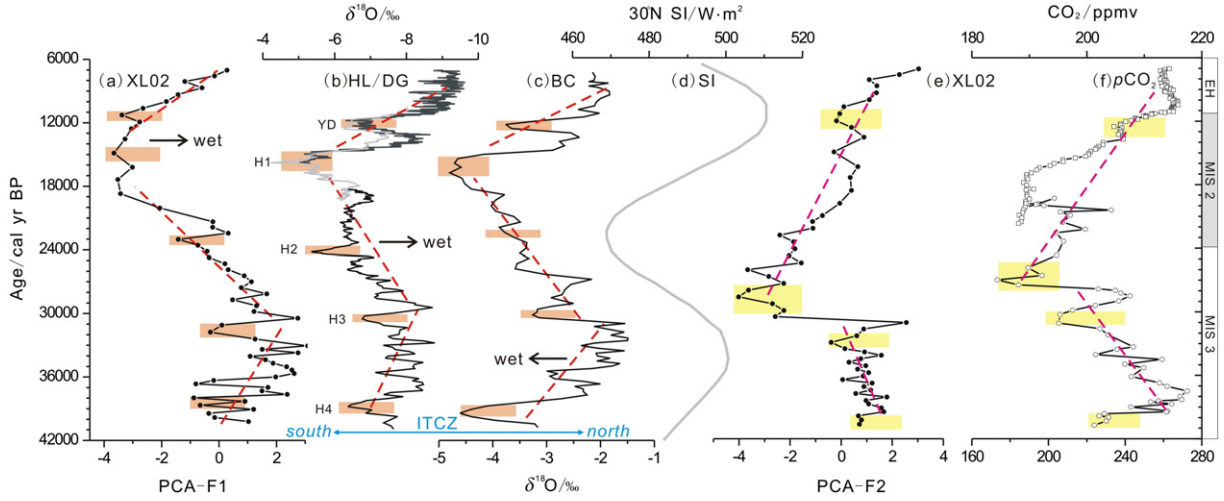

Figure 8. A comparison of summer insolation, atmospheric pCO_2 and some regional climatic proxy records. (a) Pollen PCA-F1 scores for core XL02; (b) $\delta^{18}O$ records from Hulu and Dongge Caves (HL/DG) (Wang et al., 2001; Dykoski et al., 2005) in China; (c) $\delta^{18}O$ record from Botuverá Cave (BC) in southern Brazil (Wang et al., 2007); (d) summer insolation (SI) at 30°N latitude; (e) pollen PCA-F2 scores for core XL02; (f) atmospheric pCO_2 (Monnin et al., 2004; Ahn and Brook, 2008). The shaded areas in (a), (b) and (c) indicate the YD and H1–H4 events, respectively.

https://doi.org/10.1016/j.yqres.2015.08.001 Published online by Cambridge University Press

Variations observed in the fossil pollen record from the Xialu peatland suggest that the study area probably experienced a gradual change from an open locally dense subtropical evergreen forest to a middle subtropical evergreen-deciduous mixed forest with large areas of grassland during the last glacial period, indicating that the study area experienced a wetter and warmer MIS 3 (favoring the growth of subtropical evergreen forest) and a relatively cooler and drier MIS 2 (to a certain extent promoting the local expansion of the grassland). Other proxies from the core support the climate interpretation inferred from fossil pollen data. Multi-proxy changes (Xue et al., 2014), including the LOI, OM, HD, and $\delta^{13}C_{org}$, coincide with sediment stratigraphic changes, suggesting consistently significant environmental shifts between MIS 3 and MIS 2 (Figs. 3 and 7). Unit 2, corresponding to the latter part of MIS 3, is characterized by higher LOI, OM, and HD values and more negative $\delta^{13}C_{org}$ values, which indicate a relatively wetter and warmer environment with high vegetation cover. Most of Unit 1, corresponding to MIS 2, shows lower LOI, OM, and HD values and more positive $\delta^{13}C_{org}$ values, suggesting a relatively dry and cool environment with low vegetation cover in and around the sampling site.

Comparison of reconstructed vegetation and climate with other records

The reconstruction of vegetation and climate from the Xialu peatland agrees well with many other records from Central and South China (e.g., Zheng and Lei, 1999; Zheng and Li, 2000; Wang et al., 2001; Zhong et al., 2010; Yue et al., 2012; Li et al., 2013) (Fig. 7). A previous study from eastern Guangdong Province, south China, indicated that the subtropical evergreen broad-leaf and coniferous mixed forest occupied most of the upland areas during MIS 3, consistent with a subtropical climate during this period (Zheng and Li, 2000). A more recently analyzed pollen record from the Dajiuhu peat bog (Fig. 1), central China, also indicated a relatively warmer and wetter climate during MIS 3 and a relatively colder and drier climate during MIS 2 (Li et al., 2013) (Fig. 7). Furthermore, Li et al. (2013) pointed out that the climate during the latter half of MIS 3 (prior to 24,000 cal yr BP in their record) in the Dajiuhu area was probably wetter and warmer than during early MIS 3, generally consistent with our pollen results. Multi-proxy records from the Dahu swamp in the eastern Nanling Mountains (Fig. 1), south China, also revealed a wet period between 41,000 and 27,000 cal yr BP and a marked dry and cold period from 27,000 to 17,000 cal yr BP (Zhong et al., 2010). Based on the analysis of fossil pollen obtained from the Tianyang volcanic basin in the southern Leizhou Peninsula (Fig. 1), Zheng and Lei (1999) suggested that the montane and temperate mixed forest transitioned to a Poaceae-dominated grassland, during drier and cooler climatic conditions of the LGM.

In recent years, many pollen records from the South China Sea sediments (e.g., Sun and Li, 1999; Sun et al., 2000) have been used to reconstruct paleovegetation and paleoclimate, and a series of questions focusing on the vegetation types in south China during the LGM have also arisen (Liu and Wang, 2004; Sun and Luo, 2004). For example, Sun and Li (1999) once suggested that grassland dominated by *Artemisia* (with Poaceae and Cyperaceae) occupied the exposed continental shelf of the South China Sea during the last glaciation, suggesting a cooler and drier climate during that time. However, based on a comparative study of pollen floras between two cores, a core from the Toushe Basin in central Taiwan (Liew et al., 1998) and a core from the northern slope of the South China Sea (Core 17940; Sun et al., 2000), Liu (2007) recently suggested that the regional vegetation with latitudinal distribution was subtropical evergreen broad-leaved forest in south China during the LGM. Other paleoclimate proxy records from China (An et al., 1991; Xiao et al., 1995; Chen et al., 1997; Thompson et al., 1997; Jiang and Ding, 2005), such as the $\delta^{18}O$ records from stalagmites of Hulu and Dongge caves (Wang et al., 2001; Dykoski et al., 2005), together with some other global records (Linsley, 1996; Cacho et al., 1999; Hayashi et al., 2010), are generally in agreement with our pollen results, suggesting a change from a relatively warmer and/or wetter MIS 3 to a relatively cooler and/or drier MIS 2 during the last glacial period. However, although there is a growing body of information on vegetation and climate changes in China during the late Quaternary, the patterns and mechanisms of vegetation and climate changes since the late MIS 3 (~40 ka) in different regions (e.g., South China, North China, Northwest China and the Tibetan Plateau) are still debated (Jiang et al., 2011), and the complexity of past spatial and temporal patterns of environmental change may be due to the variety of different geographic locations, topographic conditions, and complex atmospheric circulation patterns over China.

Moreover, several short excursions shown with fairly low values of AP percentages, low PCA-F1 scores, and abrupt rises in NAP percentages in our pollen data (Figs. 7 and 8) may be associated with broad-scale climatic events. For example, fluctuations at about 12,000–11,000, 18,000–15,000, 25,000–22,500, 33,000–30,500 and 39,000–37,000 cal yr BP may correspond to the Younger Dryas event (YD) and Heinrich events (H1–H4) in the North Atlantic Ocean (Heinrich, 1988; Bond et al., 1993; Grootes et al., 1993; NGRIP Members, 2004). Furthermore, a significant vegetation change, most probably reflecting a weaker summer monsoon between 29,000 and 28,000 cal yr BP, also occurred in the study area (Fig. 7), coinciding well with other records from central and eastern China (Wang et al., 2001; Li et al., 2013). Abrupt shifts similar in timing to these are clearly visible in the high-resolution stalagmite records in the EASM area as well (Wang et al., 2001). It has been suggested that these weak monsoon events were a response to cold anomalies in the North Atlantic region generated by ice-sheet disintegration (Cheng et al., 2009), because the resulting influx of meltwater and icebergs to the North Atlantic (dilute the salty water and make it less dense) could cause a shift in the location of deep-water formation and a (partial) shutdown of the meridional overturning circulation (associated northward surface-ocean transport of heat), which subsequently weaken the Asian Monsoon through atmospheric teleconnections and also move the ITCZ to the south. In addition, Xu et al. (2013) recently reported that the deglacial stage was characterized by rapid warming beginning at ~15,000 cal yr BP on land, but lagged behind marine changes by ca. 3–4 ka, consistent with the timing of the last deglacial warming in Greenland. Although our study has chronological uncertainties, a rapid warming is suggested by the pollen data from ~16,000 to 15,000 cal yr BP (Fig. 7), corresponding to the rapid strengthening of the Asian summer monsoon as reflected by $\delta^{18}O$ records of the stalagmites from Hulu Cave (Wang et al., 2001) and the last deglacial warming in the Greenland ice core (NGRIP members, 2004). Our results provide further evidence for strong climatic correlations between the northern high latitudes and low latitudes during the last glacial period.

In our previous work (Xue et al., 2014), we found a nearly inverse relationship between variations of C_3 and C_4 plant abundances reconstructed by $\delta^{13}C_{org}$ records from the Xialu peatland and Huguang Maar Lake. However, the interpretation of $\delta^{13}C_{org}$ from bulk organic sediments is complex and dependent on many factors. When $\delta^{13}C_{org}$ is viewed with the pollen results from the same core (this study), the pollen-based reconstruction of vegetation changes presented here still contrasts with that from the nearby Huguang Maar Lake (Fuhrmann et al., 2003; Mingram et al., 2004; Wang et al., 2012) (Fig. 7). Mingram et al. (2004) reported a relative environmental stability of cooler and drier conditions in the Huguang Maar Lake area between 40,000 and 15,000 cal yr BP, but there was no clear correlation with the $\delta^{18}O$ records of the stalagmites from the Hulu Cave (Wang et al., 2001) except during the Holocene. Fuhrmann et al. (2003) suggested that the NAP percentages were greater than the AP ones between 40,000 and 15,000 cal yr BP, indicating that the regional climate was cooler and drier during this time and a grassland and savanna vegetation developed—however, they provided a very low-resolution pollen record between 40.5 and 15 ka (i.e., 3000 yr per sample). A more recent pollen study showed that the Huguang Maar Lake area was dominated by subtropical evergreen forest with some deciduous trees between 40,000 and 13,000 cal yr BP, especially during the LGM; subtropical evergreen

https://doi.org/10.1016/j.yqres.2015.08.001 Published online by Cambridge University Press

forest developed but grassland vegetation did not appear (Wang et al., 2012).

While the original observations from Huguang Maar Lake are inconsistent with our present pollen records from the Xialu peatland, the results from the two studies (Fuhrmann et al., 2003; Wang et al., 2012) of vegetation types from the Huguang Maar Lake also conflict with each other. Why are there such large differences in vegetation and climate between the two neighboring regions? These contradictions are difficult to reconcile. It is still unclear if low temporal sampling resolution, age uncertainties or regional variations are responsible for these discrepancies. More detailed research is needed to resolve this extremely interesting question.

Possible driving mechanisms for evolution of vegetation communities

Previous studies have indicated that long-term Quaternary vegetation changes have been affected by climatic and environmental factors such as temperature, precipitation, and atmospheric pCO_2 levels, although the relative importance of these factors is still a subject of considerable debate (Cerling et al., 1997; Huang et al., 2001, 2006; Schefuß et al., 2003; van Asch and Hoek, 2012). The study area of the Xialu peatland is located in the transitional zone between the tropical and south subtropical subzones, and is influenced strongly by the warm/humid EASM. Fig. 8 shows that PCA-F1 broadly correlates with the $\delta^{18}O$ records of stalagmites from the Hulu and Dongge Caves in China (Wang et al., 2001; Dykoski et al., 2005) on both millennial and orbital timescales, which in turn reflect the variations of EASM intensity. This result demonstrates that vegetation changes associated with PCA-F1 were likely in response to precipitation changes resulting from the intensity of EASM, i.e. relatively stronger EASM intensity leads to higher levels of associated precipitation, and *vice versa*. The variability in PCA-F1 mirrors the $\delta^{18}O$ record of the stalagmite from the Botuverá Cave in southern Brazil (Wang et al., 2007) as well. Variations in $\delta^{18}O$ records of Chinese stalagmites and Brazilian stalagmites are generally considered good indicators of the Asian Summer Monsoon and South American Summer Monsoon, respectively, driven mainly by changes of summer insolation (Wang et al., 2001, 2005; Dykoski et al., 2005; Wang et al., 2007). However, the $\delta^{18}O$ record from southern Brazil is negatively correlated with the cave calcite records from eastern China, suggesting an interhemispheric anti-phasing of precipitation on both millennial and orbital timescales, likely related to displacement in the mean position of the ITCZ and associated asymmetry in Hadley circulation (Wang et al., 2007). Thus, the pollen data presented here, resembling different regional speleothem records (Fig. 8), suggests that the vegetation and climate in northern Leizhou Peninsula are strongly influenced by the migration of the ITCZ and changes in the EASM variability, which may be triggered by oceanic circulation changes in the high latitudes and enhanced by tropical feedbacks (Wang et al., 2007).

Furthermore, as discussed above, PCA-F2 may primarily reflect the relative changes in atmospheric pCO_2 during the last glacial period. Fig. 8 shows that PCA-F2 is generally consistent with long-term variation of atmospheric pCO_2, i.e. higher PCA-F2 values correspond to higher atmospheric pCO_2 levels, and *vice versa*. We assume that PCA-F2 mainly reflects the response of the vegetation to atmospheric pCO_2 levels during the last glacial period. Since relatively lower atmospheric pCO_2 levels could to a certain extent favor the expansion of C_4 plants (most of the non-arboreal taxa are C_4), while relatively higher atmospheric pCO_2 levels could favor the growth of C_3 plants (all arboreal taxa are C_3), although precipitation (i.e., moisture conditions) also plays a key role in the changes in relative abundance of C_3 and C_4 plants (Cerling et al., 1997; Huang et al., 2001; Schefuß et al., 2003). In our previous study, we found that atmospheric pCO_2 may have slightly affected the variations of C_3 and C_4 plant abundances on orbital time scales in Xialu peatland during the last glacial period (Xue et al., 2014). The results of the present study further suggest that the vegetation changes in the study region may be affected by variations of atmospheric pCO_2 levels both on orbital timescales and millennial timescales.

Conclusions

The fossil pollen results from the Xialu peatland presented in this study provide a well-dated record from low-latitude tropical south China since the middle of MIS 3, allowing a detailed reconstruction of last glacial vegetation and environmental dynamics in this region. The pollen data from the Xialu peatland mainly indicate three major stages of vegetation change during the interval ~40,500–7060 cal yr BP. During MIS 3 (~40,500–24,000 cal yr BP), the study region was mainly covered by subtropical evergreen trees dominated by *Altingia*, *Quercus* (E.), *Cast./Lith.* and *Sapindaceae*, indicating a subtropical climate with relatively higher temperature and precipitation in the northern Leizhou Peninsula. Under warm and wet climate conditions during the period ~30,000–25,300 cal yr BP, a significant vegetation change suggested a weaker summer monsoon between 29,000 and 28,000 cal yr BP. During MIS 2 (~24,000–11,500 cal yr BP), subtropical evergreen-deciduous broadleaved forest with large areas of grassland around the swamp occurred, implying cooler and drier conditions relative to MIS 3. A 4–5°C (or greater) decrease in MAT may have occurred in this region during this period. During the early Holocene (~11,500–7060 cal yr BP), some tropical forest elements increased, indicating a warm and wet trend into the early Holocene. Furthermore, several millennial-scale oscillations of the pollen records appear to correlate well with the known Heinrich events in the North Atlantic region, indicating strong climatic correlations between the northern high latitudes and low latitudes during the last glacial period.

The paleovegetation and paleoclimate changes in the northern Leizhou Peninsula are compatible with a model of evolution of the EASM—driven by changes of summer insolation—inferred from the $\delta^{18}O$ records of the stalagmites from China on both millennial and orbital timescales. This correlation argues that the EASM (with associated precipitation) was the major factor driving vegetation and environmental changes in the northern Leizhou Peninsula, and changes of atmospheric pCO_2 may also have had some weaker influence on vegetation changes, although other environmental factors cannot be ruled out. In addition, our pollen record indicates that the early Holocene temperature and/or precipitation may be lower than the late MIS 3. The reconstruction of vegetation and climate patterns presented here appears to be slightly different to that inferred from the neighboring Huguang Maar Lake, ~70 km east of our study site. However, these contradictions are difficult to reconcile at present and need to be further explored.

Acknowledgments

We thank Dr. Daniel Contreras at Kiel University for his language improvements. We also thank Dr. Chuanxiu Luo at the Key Laboratory of Marginal Sea Geology, CAS for her technical support. We are grateful to two anonymous reviewers and Dr. Derek B. Booth for their helpful comments and suggestions. This work was supported by the National Natural Science Foundation of China (No.41101185 and 41071137), the Specialized Research Fund for the Doctoral Program of Higher Education of China (No. 20114407120005) and the Natural Science Foundation of Guangdong Province (No. 2014A030313435).

References

Ahn, J., Brook, E.J., 2008. Atmospheric CO_2 and climate change on millennial time scales during the last glacial period. Science 322, 83–85.

An, Z.S., Kukla, G., Porter, S.C., Ziao, J., 1991. Magnetic susceptibility evidence of monsoon variation on the Loess Plateau of Central China during the last 130,000 years. Quat. Res. 36, 29–36.

Blackford, J., 2000. Palaeoclimatic records from peat bogs. Trends Ecol. Evol. 15, 193–198.

Bond, G., Broecker, W.S., Johnson, S., McManus, J., Labeyrie, L., Jouzel, J., Bonani, G., 1993. Correlations between climate records from North Atlantic sediments and Greenland ice. Nature 365, 143–147.

Bronk, R.C., 2008. Deposition models for chronological records. Quat. Sci. Rev. 27, 42–60.
Bronk, R.C., 2009. Bayesian analysis of radiocarbon dates. Radiocarbon 51 (1), 337–360.
Cacho, I., Grimalt, J.O., Pelejero, C., Canals, M., Sierro, F.J., Flores, J.A., Shackleton, N., 1999. Dansgaard-Oeschger and Heinrich event imprints in Alboran sea paleotemperatures. Paleoceanography 14, 698–705.
Cerling, T.E., Harris, J.M., MacFadden, B.J., Leakey, M.G., Quade, J., Eisenmann, V., Ehleringer, J.R., 1997. Global vegetation change through the Miocene/Pliocene boundary. Nature 389, 153–158.
Chen, F.H., Bloemendal, J., Wang, J.M., Li, J.J., Oldfield, F., 1997. High-resolution multi-proxy climate records from Chinese loess: evidence for rapid climatic changes over the last 75 kyr. Palaeogeogr. Palaeoclimatol. Palaeoecol. 130, 323–335.
Cheng, H., Edwards, R.L., Broecker, W.S., Denton, G.H., Kong, X., Wang, Y., Zhang, R., Wang, X., 2009. Ice age terminations. Science 326, 248–252.
Committee, Editorial, for Physical Geography of China, 1985. Physical Geography of China—A General Note. Science Press, Beijing (in Chinese).
Dykoski, C.A., Edwards, R.L., Cheng, H., Yuan, D.X., Cai, Y.J., Zhang, M.L., Lin, Y.S., Qing, J.M., An, Z.S., Revenaugh, J., 2005. A high-resolution, absolute-dated Holocene and deglacial Asian monsoon record from Dongge Cave, China. Earth Planet. Sci. Lett. 233, 71–86.
Fuhrmann, A., Mingram, J., Lücke, A., Lu, H.Y., Horsfield, B., Liu, J.Q., Negendank, J.F.W., Schleser, G.H., Wilkes, H., 2003. Variations in organic matter composition in sediments from Lake Huguang Maar (Huguangyan), south China during the last 68 ka: implications for environmental and climatic change. Org. Geochem. 34, 1497–1515.
Grimm, E.C., 1987. CONISS: a Fortran 77 program for stratigraphically constrained cluster analysis by the method of incremental sum of squares. Compt. Rendus Geosci. 13, 13–35.
Grootes, P.M., Stuiver, M., White, J.W.C., Johnsen, S., Jouzel, J., 1993. Comparison of oxygen isotope records from the GISP2 and GRIP Greenland ice cores. Nature 366, 552–554.
Harrison, S.P., Sanchez Goñi, M.F., 2010. Global patterns of vegetation response to millennial-scale variability and rapid climate change during the last glacial period. Quat. Sci. Rev. 29, 2957–2980.
Hayashi, R., Takahara, H., Hayashida, A., Takemura, K., 2010. Millennial-scale vegetation changes during the last 40,000 yr based on a pollen record from Lake Biwa, Japan. Quat. Res. 74, 91–99.
Heinrich, H., 1988. Origin and consequences of cyclic ice rafting in the northeast Atlantic Ocean during the past 130,000 years. Quat. Res. 29, 142–152.
Herzschuh, U., 2006. Palaeo-moisture evolution in monsoonal Central Asia during the last 50,000 years. Quat. Sci. Rev. 25, 163–178.
Huang, Y., Street-Perrott, F.A., Metcalfe, S.E., Brenner, M., Moreland, M., Freeman, K.H., 2001. Climate change as the dominant control on glacial-interglacial variations in C_3 and C_4 plant abundance. Science 293, 1647–1651.
Huang, Y., Shuman, B., Wang, Y., Webb, T., Grimm, E.C., Jacobson, G.L., 2006. Climatic and environmental controls on the variation of C_3 and C_4 plant abundances in central Florida for the past 62,000 years. Palaeogeogr. Palaeoclimatol. Palaeoecol. 237, 428–435.
Institute of Bontany and South China Institute of Bontany, 1982. Academia Sinica Angiosperm Pollen Flora of Tropic and Subtropic China. Science Press, Beijing (in Chinese).
Jiang, H.C., Ding, Z.L., 2005. Temporal and spatial changes of vegetation cover on the Chinese Loess Plateau through the last glacial cycle: evidence from spore-pollen records. Rev. Palaeobot. Palynol. 133, 23–37.
Jiang, H.C., Mao, X., Xu, H.Y., et al., 2011. Last glacial pollen record from Lanzhou (Northwestern China) and possible forcing mechanisms for the MIS 3 climate change in Middle to East Asia. Quat. Sci. Rev. 30, 769–781.
Kamenik, C., Van der Knaap, W.O., Van Leeuwen, J.F.N., Goslar, T., 2009. Pollen/climate calibration based on a near-annual peat sequence from the Swiss Alps. J. Quat. Sci. 24, 529–546.
Lambeck, K., Chappell, J., 2001. Sea level change through the last glacial cycle. Science 292, 679–686.
Li, J., Zheng, Z., Huang, K.Y., Yang, S.X., Brian, C., Verushka, V., Matthieu, C., Rachid, C., 2013. Vegetation changes during the past 40,000 years in Central China from a long fossil record. Quat. Int. 310, 221–226.
Liew, P.M., Kuo, C.M., Huang, S.Y., Tseng, M.H., 1998. Vegetation change and terrestrial carbon storage in eastern Asia during the Last Glacial Maximum as indicated by a new pollen record from central Taiwan. Glob. Planet. Chang. 16, 85–94.
Linsley, B.K., 1996. Oxygen-isotope record of sea level and climate variations in the Sulu Sea over the past 150,000 years. Nature 380, 234–237.
Liu, J.L., 2007. Additional remarks on vegetation types in south China during the last glacial maximum (LGM). Acta Microbiol. Sin. 24 (1), 105–112 (in Chinese).
Liu, J.L., Wang, W.M., 2004. A discussion on the vegetation types during LGM time in south China. Quat. Sci. 24 (1), 213–216 (in Chinese).
Mingram, J., Schettler, G., Nowaczyk, N., Luo, X.J., Lu, H.Y., Liu, J.Q., Negendank, J., 2004. The Huguang Maar Lake—a high-resolution record of palaeoenvironmental and palaeoclimatic changes over the last 78,000 years from South China. Quat. Int. 122, 85–107.
Mix, A.C., Bard, E., Schneider, R., 2001. Environmental processes of the ice age: land, oceans, glaciers (EPILOG). Quat. Sci. Rev. 20, 627–657.
Monnin, E., Steig, E.J., Siegenthaler, U., Kawamura, K., Schwander, J., Stauffer, B., Stocker, T.F., Morse, D.L., Barnola, J.M., Bellier, B., Raynaud, D., Fischer, H., 2004. Evidence for substantial accumulation rate variability in Antarctica during the Holocene through synchronization of CO_2 in the Taylor Dome, Dome C and DML ice cores. Earth Planet. Sci. Lett. 224, 45–54.
Nakagawa, T., Brugiapaglia, E., Digerfeldt, G., Reille, M., de Beaulieu, J.L., Yasuda, Y., 1998. Dense-media separation as a more efficient pollen extraction method for use with organic sediment samples: comparison with the conventional method. Boreas 25, 15–24.
North Greeland Ice Core Project members (NGRIP members), 2004. High resolution climate record of the Northern Hemisphere back into the last Interglacial period. Nature 431, 147–151.
Petertson, G.M., Webb, T., Kutzbach, J.E., van der Hammen, T., Wijmstra, T.A., Street, F.A., 1979. The continental record of environmental conditions at 18,000 yr B.P.: an initial evaluation. Quat. Res. 12, 47–82.
Reimer, P.J., Bard, E., Bayliss, A., Beck, J.W., Blackwell, P.G., Bronk Ramsey, C., Brown, D.M., Buck, C.E., Edwards, R.L., Friedrich, M., Grootes, P.M., Guilderson, T.P., Haflidason, H., Hajdas, I., Hatte, C., Heaton, T.J., Hogg, A.G., Hughen, K.A., Kaiser, K.F., Kromer, B., Manning, S.W., Reimer, R.W., Richards, D.A., Scott, E.M., Southon, J.R., Turner, C.S.M., van der Plicht, J., 2013. Selection and treatment of data for radiocarbon calibration: an update to the International Calibration (INTCAL) Criteria. Radiocarbon 55 (4), 1–23.
Schefuß, E., Schouten, S., Jansen, J.H., Damsté, J.S., 2003. Africa vegetation controlled by tropical sea surface temperatures in the mid-Pleistocene period. Nature 422, 418–421.
Siddall, M., Rohling, E.J., Thompson, W.G., Waelbroeck, C., 2008. Marine isotope stage 3 sea level fluctuations: data synthesis and new outlook. Rev. Geophys. 46, RG4003.
Sun, X.J., Li, X., 1999. A pollen record of the last 37 ka BP in deep core 17940 from the northern slope of the South China Sea. Mar. Geol. 156, 227–244.
Sun, X.J., Luo, Y.L., 2004. From pollen record to paleovegetation: reply to "A discussion on the vegetation types during LGM time in south China". Quat. Sci. 24 (2), 217–221 (in Chinese).
Sun, X.J., Li, X., Luo, Y.L., Chen, X.D., 2000. The vegetation and climate at the last glaciation on the emerged continental shelf of the South China Sea. Palaeogeogr. Palaeoclimatol. Palaeoecol. 160, 301–316.
Tang, Q.Y., Zhang, C.X., 2013. Data Processing System (DPS) software with experimental design, statistical analysis and data mining developed for use in entomological research. Insect Sci. 20, 254–260.
Thompson, L.G., Yao, T.D., Davis, M.E., Henderson, K.A., Mosley-Thompson, E., Lin, P.N., Beer, J., Synal, H.A., Cole-Dai, J., Bolzan, J.F., 1997. Tropical climate instability: the last glacial cycle from a Qinghai–Tibetan ice core. Science 276, 1821–1825.
Van Asch, N., Hoek, W.Z., 2012. The impact of summer temperature changes on vegetation development in Ireland during the Weichselian Lateglacial Interstadial. J. Quat. Sci. 27, 441–450.
Wang, F.S., Chien, N.F., Zhang, Y.L., Yang, H.Q., 1995. Pollen Flora of China. Second edition. Science Press, Beijing (in Chinese).
Wang, Y.J., Cheng, H., Edwards, R.L., An, Z.S., Wu, J.Y., Shen, C.C., Dorale, J.A., 2001. A high-resolution absolute-dated late Pleistocene monsoon record from Hulu Cave, China. Science 294, 2345–2348.
Wang, Y.J., Cheng, H., Edwards, R.L., He, Y.Q., Kong, X.G., An, Z.S., Wu, J.Y., Kelly, M.J., Dykoski, C.A., Li, X.D., 2005. The Holocene Asian monsoon: links to solar changes and North Atlantic climate. Science 308, 854–857.
Wang, X., Auler, A.S., Edwards, R.L., Cheng, H., Ito, E., Wang, Y., Kong, X.G., Solheid, M., 2007. Millennial-scale precipitation changes in southern Brazil over the past 90,000 years. Geophys. Res. Lett. 34, L23701.
Wang, S.Y., Lu, H.Y., Han, J.T., Chu, G.Q., Liu, J.Q., Negendank, F.W., 2012. Palaeovegetation and palaeoclimate in low-latitude southern China during the Last Glacial Maximum. Quat. Int. 248, 79–85.
Xiao, J., Porter, S.C., An, Z.S., Kumai, H., Yoshikawa, S., 1995. Grain size of quartz as an indicator of winter monsoon strength on the Loess Plateau of Central China during the last 130,000 yr. Quat. Res. 43, 22–29.
Xu, D.K., Lu, H.Y., Wu, N.Q., Liu, Z.X., Li, T.G., Shen, C.M., Wang, L., 2013. Asynchronous marine-terrestrial signals of the last deglacial warming in East Asia associated with low- and high-latitude climate changes. Proc. Natl. Acad. Sci. U. S. A. 110, 9657–9662.
Xue, J.B., Zhong, W., Cao, J.Y., 2014. Changes in C_3 and C_4 plant abundances reflect climate changes from 41,000 to 10,000 years ago in northern Leizhou Peninsula, South China. Palaeogeogr. Palaeoclimatol. Palaeoecol. 396, 173–182.
Yu, K.F., Zhong, J.L., Zhao, J.X., Shen, C.D., Chen, T.G., Zhong, J.L., Zhao, H.T., Song, C.J., 2002. Biological-geomorphological zones in a coral reef area at southwest Leizhou Peninsula unveil multiple sea level high-stands in the Holocene. Mar. Geol. Quat. Geol. 22, 27–33 (in Chinese).
Yue, Y.F., Zheng, Z., Huang, K.Y., Manuel, C., Brian, C., Matthieu, C., Marie-Pierre, L., Rachid, C., 2012. A continuous record of vegetation and climate change over the past 50,000 years in the Fujian Province of eastern subtropical China. Palaeogeogr. Palaeoclimatol. Palaeoecol. 365–366, 115–123.
Zhao, Y., Yu, Z.C., Zhao, W.W., 2011. Holocene vegetation and climate histories in the eastern Tibetan Plateau: controls by insolation-driven temperature or monsoon-derived precipitation changes? Quat. Sci. Rev. 30, 1173–1184.
Zheng, Z., Lei, Z.Q., 1999. A 400,000 year record of vegetational and climatic changes from a volcanic basin, Leizhou Peninsula, southern China. Palaeogeogr. Palaeoclimatol. Palaeoecol. 145, 339–362.
Zheng, Z., Li, Q.Y., 2000. Vegetation, climate, and sea level in the past 55,000 years, Hanjiang Delta, Southeastern China. Quat. Res. 53, 330–340.
Zhong, W., Ma, Q.H., Xue, J.B., Zheng, Y.M., Cai, Y., OuYang, J., 2010. Humification degrees of a limnologic sediment sequence in eastern Nanling Mountains as an indicator of past climatic changes in the last c.49,000 years in South China. Boreas 39, 286–295.
Zhou, W.J., Yu, X.F., Timothy, Jull A.J., Burr, G., Xiao, J.Y., Lu, X.F., Xian, F., 2004. High-resolution evidence from southern China of an early Holocene optimum and a mid-Holocene dry event during the past 18,000 years. Quat. Res. 62, 39–48.

https://doi.org/10.1016/j.yqres.2015.08.001 Published online by Cambridge University Press